Journal of Applied Microbiology, 2025, 136(7), lxaf155
https://doi.org/10.1093/jambio/lxaf155
Advance access publication date: 23 June 2025
Research Article

JOURNAL OF APPLIED MICROBIOLOGY
OXFORD UNIVERSITY PRESS

2-hydroxy-dibenzylideneacetone as a multifunctional coating inhibiting biofilm formation of *Candida albicans*

Veridianna C. Pattini[1,2], Leticia R. de Assis[2], Margarete T. G. de Almeida[3], Luis O. Regasini[2], Henny C. van der Mei[1,*]

[1]University of Groningen and University Medical Center Groningen, Department of Biomaterials and Biomedical Technology, 9713 AV Groningen, The Netherlands
[2]São Paulo State University (UNESP), Institute of Biosciences, Humanities and Exact Sciences (Ibilce), São José do Rio Preto, São Paulo 15054-000, Brazil
[3]São José do Rio Preto Medical School (Famerp), São José do Rio Preto, São Paulo 15090-000, Brazil
*Corresponding author. University Medical Center Groningen, Antonius Deusinglaan 1, 9713 AV Groningen, The Netherlands. E-mail: h.c.van.der.mei@umcg.nl

Abstract

Aim: *Candida albicans* emerges as an opportunistic fungus among nosocomial infections, which can include sepsis, bloodstream infections, and infections associated with medical devices. Therefore, we investigated the effectiveness of 2-hydroxy-dibenzylideneacetone, a monocarbonyl curcuminoid, as an antifouling coating against *C. albicans*.

Methods and results: Polystyrene (hydrophobic) and glass (hydrophilic) were used to study the influence of a curcuminoid coating on biofilm formation. Fourier-transform-infrared-spectroscopy spectra indicated a successful curcuminoid coating on both surfaces. Atomic-force-microscopy data showed that the curcuminoid coating on polystyrene decreased the adhesion strength of *C. albicans* but had minimal effect on glass. Hyphal growth, a key virulence factor, was significantly reduced on both coated surfaces. Biofilm formation was significantly reduced on coated polystyrene, but not on glass. Gene expression revealed downregulation of adhesion and biofilm-related genes (*HWP1, ALS3, ALS5*). Exposure of a 48-h biofilm to curcuminoid decreased the metabolic activity of the biofilm. The curcuminoid coating was biocompatible and non-cytotoxic against human oral keratinocytes and human gingival fibroblasts.

Conclusions: This study underscores the potential of a curcuminoid coating to prevent *C. albicans* adhesion, reduce hyphal and biofilm formation, and reduce metabolic activity of biofilms, highlighting its potential use as an antifouling coating against *Candida*-associated infections.

Impact Statement:

This study highlights the potential of a curcuminoid-based coating to mitigate *C. albicans* biofilm formation on various materials by reducing fungal adhesion, inhibiting hyphal formation, and downregulating of biofilm-related genes. Therefore, this coating presents a promising antifouling strategy against *Candida*-associated infections. These findings offer valuable insights for developing novel surface modifications to enhance the safety and durability of biomaterials.

Keywords: anti-fouling; anti *candida*; curcumin; antifungal; surface modifications

Introduction

Biofilms are life-threatening in medical-related infections, particularly when associated with medical devices, such as intravascular and urinary catheters, dental implants, orthopaedic implants, and artificial heart valves (Srivastava et al. 2019). Once microorganisms are attached to surfaces, they can form microcolonies and induce metabolic, phenotypic, and genotypic alterations, leading to increased microbial resistance to antimicrobial agents when compared to planktonic cells (Singh et al. 2019). The extracellular matrix of biofilms provides structural protection, shielding the embedded microorganisms from both antimicrobial treatments and host immune responses (Singh et al. 2019). Additionally, biofilms adhere strongly to medical implants and devices, making their complete eradication difficult without device removal or aggressive treatment strategies. Even if biofilm burden is temporarily reduced, dormant cells within the biofilm can survive treatment, leading to recurrent infections and complicating patient management (Srivastava et al. 2019). *Candida albicans* emerges as the most frequent opportunistic fungus among nosocomial infections, accounting for 15% of sepsis and 40% of bloodstream infections in clinical settings, being one of the most prevalent causative agents of bloodstream infections associated with vascular devices in hospital settings (Pfaller and Diekema 2007, Magill et al. 2014). Hence, the elimination of biofilms presents a challenge within the medical field. Due to its clinical relevance as an opportunistic pathogen responsible for biofilm-associated infections, particularly in immunocompromised patients, *C. albicans* was chosen for this work.

Currently, studies are focused on exploring surface modifications to create antifouling materials for medical devices and implants by an antimicrobial coating or an antimicrobial releasing coating to prevent or disrupt the adhesion of microorganisms and inhibit biofilm formation on medical devices and implants (Abreu et al. 2013, Campoccia et al. 2013). Antifungal agents such as amphotericin (Alves et al. 2019), fluconazole (Naderi et al. 2020), and caspofungin (Lamont-Friedrich et al. 2021) have demonstrated promising outcomes.

Received 3 April 2025; **revised** 4 June 2025; **accepted** 22 June 2025

Table 1. Molecular structures of monocarbonyl curcuminoids **A-G**.

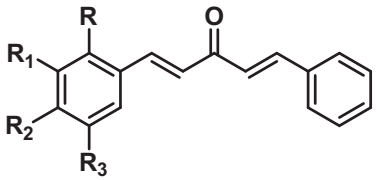

Monocarbonyl curcuminoid	Code	R	R_1	R_2	R_3	References
3,5-dimethoxy-4-hydroxy-dibenzylideneacetone	**A**	H	OCH_3	OH	OCH_3	This paper
3-methoxy-4-hydroxy- dibenzylideneacetone	**B**	H	OCH_3	OH	H	Weber et al. 2005, Polaquini et al. 2021
3-hydroxy-4-methoxy- dibenzylideneacetone	**C**	H	OH	OCH_3	H	Polaquini et al. 2024
2-hydroxy-dibenzylideneacetone	**D**	OH	H	H	H	Dai et al. 2015, Shen et al. 2015
3-hydroxy-dibenzylideneacetone	**E**	H	OH	H	H	Dai et al. 2015, Shen et al. 2015, Polaquini et al. 2021, Polaquini et al. 2024
4-hydroxy-dibenzylideneacetone	**F**	H	H	OH	H	Zhou et al. 2018, Polaquini et al. 2021
2,5-dihydroxy-dibenzylideneacetone	**G**	OH	H	H	OH	Polaquini et al. 2024

However, their persistent application on surfaces can contribute to the selection and emergence of novel resistant strains. Consequently, innovative strategies are being explored to develop antimicrobial biomaterials that do not rely on antibiotic release (Afewerki et al. 2020).

Curcumin has shown promising potential as an antimicrobial product to coat materials with applications, from the food industry (Manohar et al. 2015) to the healthcare sector, in wound dressings (Gaydhane et al. 2020) and coatings on medical devices, such as surgical sutures, which showed faster healing and less inflammation of the wound in a mouse model (Sunitha et al. 2017). Multilayer curcumin-loaded coatings have exhibited sustained release and strong antibacterial effects, confirming their suitability for orthopaedic implants (Virk et al. 2019). Additionally, a coating mixture of curcumin, chlorhexidine, and silver has proven effective for urinary catheters, demonstrating prevention and inhibition of bacterial colonization, along with lubricious properties (Modak et al. 2019). However, a silver-based coating has, besides their broad-spectrum antimicrobial activity, concerns about their cytotoxicity and the potential for ion release into surrounding tissues, which can cause collateral damage (Duval et al. 2019, Thapliyal et al. 2025). Other coatings like chitosan-based coatings, offer a good biocompatibility and intrinsic antifungal activity, though their mechanical stability and long-term performance may be limited under physiological conditions (Kumari et al. 2021). Natural curcumin also presents a limitation associated with its stability under physiological conditions preventing its clinical use (Nelson et al. 2017). The β-diketone moiety replacement in the curcumin by a monocarbonyl has overcome this limitation and improved its bioactivities (Shetty et al. 2014). The antifungal effect of monocarbonyl curcumin analogues has been little explored. Only a few papers describe their antifungal activity, in which they only searched a preliminary susceptibility assay against planktonic yeast cells (Nagargoje et al. 2020a, b).

Understanding the mechanisms of action of monocarbonyl curcuminoids as antifungal agents and exploring their potential as a coating on materials can lead to innovative approaches in combating *Candida* biofilm-associated infections. According to former literature, there are no investigations focused on coating surfaces with monocarbonyl curcumin analogues. Polystyrene and glass were selected as model materials to represent extremes of hydrophobicity and hydrophilicity, respectively. The aim of this study is to investigate if monocarbonyl curcuminoids can be used as a coating on the surface in order to avoid biofilm formation and pave the way for future investigations into how surface properties influence *C. albicans* adhesion and biofilm formation.

Materials and methods

Curcumin and monocarbonyl curcuminoids

Curcumin and all reagents and solvents were purchased from Merck (Kenilworth, USA). The syntheses of monoketone curcuminoids **A**–**G** (Table 1) were performed using the procedures described by Polaquini et al. (2021, 2024). The structures of the compounds were confirmed by ^{1}H and ^{13}C NMR spectral data analyses (Figs S1–S7) (Weber et al. 2005, Dai et al. 2015, Shen et al. 2015, Zhou et al. 2018).

Fungal strains, harvesting, and culture conditions

Reference strains, including *C. albicans* ATCC 10231, *Candida krusei* ATCC 40147 (these strains were purchased from the American Type Culture Collection, USA), *Candida auris* CBS 10913 (this strain was purchased from Centraalbureau voor Schimmelcultures, The Netherlands) and clinical isolates, including *C. albicans* 6293 (genital tract infection) and *C. auris* CAU 491 (systemic infection) were used for the susceptibility tests. The clinical strains were obtained from the collection of the Laboratory of Mycology, Department of Dermatological, Infectious, and Parasitic Diseases, São José do Rio Preto Medical School (FAMERP), São José do Rio Preto, Brazil. The strains were grown on Sabouraud Dextrose Agar (Difco Laboratories, Detroit, MI, USA), and yeast colonies from the agar were suspended in phosphate-buffered saline (PBS, 5 mmol l^{-1} K_2HPO_4, 5 mM KH_2PO_4, and 0.15 M NaCl, pH 7.0) to a concentration of 3×10^6 yeasts ml^{-1}, as determined in a Bürker-Türk counting chamber.

To prepare yeast suspensions for the adhesion and atomic force microscopy experiments, one colony from the agar plate was transferred into 10 ml yeast nitrogen base (YNB, Difco Laboratories, Detroit, MI, USA) and grown for 24 h at 30°C. This pre-culture was inoculated in 190 ml YNB (1:20), and the main culture was grown for 16 h at 30°C. Yeast was harvested by centrifugation for 5 min at 4000 × *g* and resuspended in 10 ml PBS, this was repeated three times to remove all traces

of growth medium. Finally, yeast was resuspended in PBS to a concentration of 3×10^6 ml^{-1}.

Susceptibility assay to determine the most active curcuminoids

To select the most active curcuminoid, the susceptibility profile of *Candida* spp. against the curcuminoids was measured by determining the minimum inhibitory concentrations (MIC) and minimum fungicidal concentrations (MFC), according to the Clinical Laboratory Standard Institute (CLSI) document M27-A3 (CLSI 2008), with some minor modifications. Briefly, the yeast suspension was diluted to 3×10^3 ml^{-1} in RPMI-1640 medium (Rosen Park Media Institute, Sigma-Aldrich, St. Louis, MO, USA), and 100 μl of the yeast suspension was added to a 96 wells polystyrene plate containing 100 μl RPMI-1640 medium with different concentrations of the curcuminoids (500−7.8 μg ml^{-1}). RPMI-1640 medium was the negative control, and yeast suspension without curcuminoids was the positive control. The plates were incubated at 30°C for 24 h. The MIC value was determined as the lowest concentration with no visible growth. To determine MFC, an aliquot of 10 μl from each well without visible growth was plated on Sabouraud Dextrose Agar and incubated at 30°C for 24 h. The MFC was defined as the lowest concentration of the curcuminoid showing no colonies on the agar plates. The experiment was performed in triplicate with separately cultured yeast. The most active compound, 2-hydroxy-dibenzylideneacetone (**D**), was selected for further studies described below.

Coating surfaces with curcuminoid **D**

Hydrophobic polystyrene and hydrophilic glass were used as model materials because these materials are easy and convenient to use. They are stable over time, non-toxic, transparent, which has the advantage of live imaging by microscopy, easy to manufacture, and have low production cost. In addition, polystyrene has a similar hydrophobicity and roughness with polymeric materials used for medical devices, such as silicone rubber used for catheters and voice prostheses. Sterile 12, 48, and 96-well polystyrene flat-bottom microtiter plates were purchased from CELLSTAR® (Greiner Bio-One, Frickenhausen, Germany), and microscope glass slides from Epredia (Thermo Scientific, Portsmouth, NH, USA). All glass disks were cleaned by sonication for 5 min in 2% RBS 35 detergent (Omnilabo International BV, The Netherlands), rinsed with tap water, washed in methanol (Merck, Darmstadt, Germany), and washed with sterile demineralized water.

The curcuminoid **D** was diluted at 2 mg ml^{-1} in YNB + DMSO (10%). For coating the polystyrene well plates, 100 µl of the curcuminoid solution was added to each well in a 96 wells plate, 400 µl for 48 wells plate, and 800 µl for 12 wells plate. Glass slides (25 × 75 mm) were exposed to 5 ml of the curcuminoid solution, and the smaller glass slides (15 × 15 mm) to 800 µl of the curcuminoid solution. The glass disks (8 mm in diameter) were exposed to 400 µl of the curcuminoid solution. All surfaces were exposed for 24 h at 25 °C, followed by thorough washing with PBS buffer to remove unbound curcuminoid.

Surface characterization of curcuminoid coatings

The chemical structure of curcuminoid **D** coated on polystyrene and glass surfaces was determined using Fourier transform infrared (FTIR) spectroscopy. FTIR spectra were measured on an Agilent Cary 600 series FTIR spectrometer (Agilent Technologies, St. Clara, CA, USA). FTIR spectra were recorded over the wavenumber range of 4000 and 400 cm^{-1} with a resolution of 4 cm^{-1}, and 32 scans were measured and averaged.

Water contact angles were measured to determine the hydrophilicity of the curcuminoid-coated and uncoated polystyrene and glass slides. Water contact angle measurements were carried out using the sessile drop technique with ultrapure water. Ultrapure water droplets of 2 µl were placed on the surfaces and observed using an Olympus BX-41 microscope objective lens. The images were digitally captured using a 1.4-megapixel CCD camera, and the contact angle was measured with an image analysis software program (MATLAB, MathWorks, Natick, MA, USA). The reported water contact angles are means of five measurements performed on different areas of each sample surface in three separate experiments.

The influence of curcuminoid coating on *C. albicans* adhesion in a parallel plate flow chamber

The adhesion of *C. albicans* ATCC 10231 was monitored on uncoated and curcuminoid **D** coated glass slides on the bottom plate of a parallel plate flow chamber, as described previously (Busscher and Van Der Mei 2006). The adhesion of *C. albicans* (10^6 cells ml^{-1}) in PBS was observed with a phase-contrast microscope (Olympus BH-2) equipped with a 10 × ultra-long working distance objective (Olympus ULWD-CD Plan 40 PL), connected to a CCD-MXRi camera (Basler A101F, Basler AG, Germany). After 4 h of flowing (share rate of 15 s^{-1}) the yeast suspension through the flow chamber, images were taken at 10 different locations on each sample. The yeast suspension was drained to determine the adhesion strength of the yeasts using an air-liquid interface over the adhering yeast, and the flow chamber was filled again with PBS to take images at 10 different locations. The number of adhering yeasts obtained on the curcuminoid coating was compared to the uncoated glass.

Image analysis was done using software based on the Matlab Image Processing Toolkit (The MathWorks, MA, USA). Live images were acquired after the summation of 15 consecutive images (time interval 1 s) to enhance the signal-to-noise ratio and to eradicate flowing yeast from the analysis. The experiments were done in triplicate with separately cultured yeasts.

Adhesion strength of yeasts on curcuminoid-coated surfaces using atomic force microscopy

The adhesion forces of *C. albicans* ATCC 10231 on uncoated and curcuminoid **D** coated polystyrene and glass were measured using atomic force microscopy, as described previously (Carniello et al. 2020). Before each measurement, cantilevers (Bruker, Billerica, MA, USA) were calibrated using the thermal tuning method, and spring constants were always close to the producer's specification of 0.06 N m^{-1}. The yeast probe was prepared by immobilizing a yeast cell to an NP-0 tipless cantilever coated with poly-L-lysine (Sigma-Aldrich, St. Louis, MO, USA) using electrostatic interaction. Yeast probes were used immediately after the preparation. All adhesion forces were performed in PBS at room temperature under a loading force of 5 nN and at three randomly chosen spots on uncoated and curcuminoid-coated polystyrene and glass. The experiments were performed in duplicate with separately cultured yeasts.

The influence of curcuminoid coating on hyphal development of *C. albicans*

The hyphal development was performed on uncoated and coated polystyrene 12 wells plate and glass slides (15 × 15 mm). In each well with or without glass slides and with or without a curcuminoid **D** coating, 800 µl *C. albicans* (10^4 cells ml^{-1}) in YNB were added and incubated for 3.5 h with shaking (80 rpm) at 37°C. After 3.5 h, the hyphal development was analysed using an inverted microscope (Rebel, RBLTEW31) equipped with an iPad Pro 2 MP CMOS colour camera. Three pictures of each well were taken in each experiment. The experiment was performed in triplicate with separately cultured yeasts.

The efficacy of curcuminoid coating on biofilm formation

The biofilm formation was performed on uncoated and coated polystyrene 48 wells plate and glass disks (8 mm in diameter). In each well with or without a glass disk and with or without a curcuminoid coating, 400 µl *C. albicans* (10^6 cells ml^{-1}) in PBS was added and incubated at 37°C under shaking at 80 rpm for 2 h. After 2 h, the PBS was removed, and 400 µl of Sabouraud Dextrose Broth was added to the wells. The plate was incubated under the same conditions for 48 h. The culture medium was refreshed after 24 h. After 48 h, the growth medium was removed, and the biofilm was washed carefully twice with 400 µl PBS to remove non-attached cells, and the glass disks were removed from the 48-well plate and transferred to a clean well. To the wells with or without a glass disk 400 µl of PBS was added. The plate was sealed with Parafilm and sonicated for 5 min to detach the biofilm from the polystyrene and glass disk surfaces. After sonication, the biofilm was suspended using a pipette. Sequential dilutions were performed, and three 10 µl aliquots from each well were plated on Sabouraud Dextrose Agar and incubated at 30°C for 24 h, after which the colony forming units (CFUs) were counted. The experiment was performed in triplicate with separately cultured yeasts.

In order to evaluate the therapeutic effect of curcuminoid **D**, 100 µl of *C. albicans* (10^6 cells ml^{-1}) in PBS was added in each well of a polystyrene 96 wells plate and incubated at 37°C under shaking at 80 rpm for 2 h. After 2 h, the PBS was removed, and 100 µl of Sabouraud Dextrose broth was added to the wells. The plate was incubated under the same conditions for 48 h, and the culture medium was refreshed after 24 h. After 48 h and removal of the culture medium, curcuminoid **D** diluted in Sabourand Dextrose broth and 10% DMSO, was added into the wells with the biofilm at different concentrations (0, 31.2, 62.5, 156, and 312 µg ml^{-1}) and incubated under the same conditions for 24 h. After incubation, the growth medium was removed, and the biofilms were washed with PBS to remove non-adhered cells. The metabolic activity of the biofilms was determined with 3-(4,5-dimethylthiazol-2-yl)-2,5-diphenyl tetrazolium bromide (MTT), a yellow dye, which is reduced by cellular enzymes to the blue formazan. Briefly, 100 µl of MTT solution (1 mg ml^{-1} in PBS) was added to each well of a 96 wells plate with a biofilm and incubated at 37°C for 4 h, protected from light. After 4 h, the MTT solution was removed, and the plates were air dried, and 100 µl of 2-propanol was added to dissolve the MTT-formazan product. 100 µl of the propanol-solubilized product was transferred to a new 96-well plate, and the optical density was measured at 570 nm on a microplate reader. All data were expressed relative to biofilms exposed to only growth medium.

Confocal laser scanning microscopy (CLSM, Leica) was used to visualize 48 h biofilms of *C. albicans* ATCC 10231 grown on curcuminoid coated and uncoated polystyrene and glass surfaces. After 48 h, biofilms were washed with PBS and stained with the LIVE/DEAD™ Yeast Viability Kit (Invitrogen, ThermoFisher Scientific, The Netherlands). The Kit was provided with two stains: FUN-1 and Calcofluor White M2R. Upon excitation, FUN-1 shows green fluorescent membrane structures and red fluorescent metabolically active intravacuolar structures, and Calcofluor white stains cell walls blue fluorescent. Staining was done according to the manufacturer's instructions, after which excess stain was removed by washing two times with PBS, and biofilms were immersed in 3 ml PBS. CLSM images were collected using a Leica TCS SP2 CLSM with a 40x water objective using 580 nm excitation and emission filter settings of 365–510 (blue, cell wall), 510–560 nm (green, membrane), and 560–610 nm (red, metabolically active intravacuolar structures). Images were taken over the depth of a biofilm in sequential z-intervals of 2 µm. Subsequently, the stacks of images acquired were colour-coded and quantitatively analysed using fully open-source and free software (Fiji/ImageJ).

Analysis of the influence of curcuminoid coatings on the gene expression of *C. albicans* biofilms

The gene expression analyses were performed at different stages of biofilm formation after 2 h and 48 h biofilm growth and after hyphal development in order to evaluate the interference of the curcuminoid **D** coating with the genes responsible for adhesion, aggregation, and hyphal development of *C. albicans*. The genes analysed were: *ALS1* (agglutinin-like sequence 1), *ALS3* (agglutinin-like sequence 3), *ALS5* (agglutinin-like sequence 5), and *HWP1* (hyphal cell wall protein 1), and *ACT1* (Actin 1) was used as the household gene.

The different stages of biofilm formed on coated and uncoated polystyrene surfaces were suspended in PBS prepared in ultrapure water (DNA/RNA free) and subjected to centrifugation for 2 min at 12 000 × *g*, and the supernatant was discarded from the pellet. RNA was extracted from the yeasts using the RiboPure RNA Purification Kit, Yeast (Invitrogen, Thermo Fisher Scientific, Groningen, The Netherlands) according to the manufacturer's instructions. Traces of genomic DNA were removed using the DNA-free kit (Invitrogen, Thermo Fisher Scientific, Groningen, The Netherlands). The amount and quality of extracted RNA were based on the 260/280-nm ratio measured using the NanoDrop ND-1000 (NanoDrop Technologies LLC, Thermo Fisher Scientific, Wilmington, DE, USA). A mixture of 200 ng RNA, 4 µl 5 × iScript reaction mixture, and 1 µl iScript reverse transcriptase, in a total volume of 20 µl (iScript; Bio-Rad, Hercules, CA), was used for cDNA synthesis according to the manufacturer's instructions. Real-time reverse transcription-quantitative PCR (RT-qPCR) was performed in a 384-well plate (HSP-3905; Bio-Rad Laboratories, Foster City, CA, USA) with the primer sets for the selected genes (see Table S1 in the supplementary material). The following thermal conditions were used for all RT-qPCRs: 95°C for 3 min and 40 cycles of 95°C for 15 s and 60°C for 45 s.

The absolute C_t values from all the RT-qPCR assays were used to calculate the expression ratios of the genes in

C. albicans cells formed on curcuminoid-coated glass and polystyrene surfaces compared to uncoated counterparts. The values obtained were normalized using the household *ACT1* (encoding beta-actin) gene as a reference. The data were expressed in relation to the gene expression of the positive control (biofilms formed on uncoated surfaces). Gene expression was assessed in triplicate experiments with separately grown cultures.

Evaluation of the cytotoxicity of curcuminoid-coated polystyrene surfaces on human cells

Human gingival fibroblast (HGF-1 CRL-2014; ATCC, USA) and human oral keratinocytes (HOK, CellSystems, Germany) were used for cytotoxicity evaluation. HGF-1 cells were grown in Dulbecco's Modified Eagle's Medium containing 4.5 g l^{-1} glucose (DMEM-HG; Gibco, USA) supplemented with 10% foetal bovine serum (FBS; Gibco, USA), and HOK cells were grown in keratinocyte growth medium complete (CellSystems, Germany), and both cells were grown in a humidified incubator at 37°C with 5% CO_2. After growth till 70–90% confluency, cells were trypsinized for harvesting using centrifugation, adjusted to a final concentration of 2.5×10^4 cells ml^{-1}, and 100 μl was seeded to each well of a 96 well plate pre-coated with curcuminoid, and uncoated wells were used as control. After 24 h of exposure to curcuminoid-coated surface, cell viability was evaluated by XTT assay (Thermo Fisher Scientific, USA) using the manufacturer guidelines. Briefly, 50 µl of activated XTT reagent was added to the well and incubated for another 2 h (37°C, 5% CO_2). Absorbances were measured by a plate reader with dual wavelengths at 450 nm and at 660 nm as reference. Uncoated wells were used as controls for measuring the cell viability, and wells with only culture media and activated XTT reagent were used as blank controls.

Statistical analysis

Statistical analysis was performed using GraphPad Prism Software (version 8.2 for Windows, La Jolla, California, USA). Data are the mean of three biologically independent experiments ± standard deviation (SD). Statistically significant differences between the experimental groups were determined by one-way analysis of variance (ANOVA) or Student's *t*-test. A *P*-value of $\leq .05$ was considered statistically significant.

Results

MIC and MFC of curcuminoids

The anti-*Candida* activities of curcumin and unsymmetrical monocarbonyl analogues (Curcuminoids **A-G**) were evaluated against six *Candida* strains (Table 2). Out of seven curcumin analogues, six compounds inhibited the growth of at least one *Candida* strain at concentrations below 250 µg ml^{-1} (Table 2). The hydroxyl group position was particularly relevant for fungitoxicity, compounds with hydroxyl groups at the carbons 2′ (**D**) and 3′ (**C**) exhibited higher anti-*Candida* activity compared to their regioisomer at carbon 4′ (**F**) position. This pattern was also observed in methoxylated-hydroxylated curcuminoids, as curcuminoid **C**, with hydroxyl at position 3′ and methoxyl at position 4′, which inhibited three strains. On the other hand, curcuminoid **B** with methoxyl and hydroxyl at position 3′ and 4′, respectively, did not inhibit growth of any

Table 2. Antifungalactivity of curcuminoids against planktonic *Candida* species determined by MIC and MFC.

Compounds	R	*C. albicans* ATCC 10 213		*C. albicans* 6293		*C. krusei* ATCC 40 147		*C. auris* CBS 10 913		*C. auris* CAU 491	
		MIC (µg ml^{-1})	MFC (µg ml^{-1})	MIC (µg ml^{-1})	MFC (µg ml^{-1})	MIC (µg ml^{-1})	MFC (µg ml^{-1})	MIC (µg ml^{-1})	MFC (µg ml^{-1})	MIC (µg ml^{-1})	MFC (µg ml^{-1})
Curcumin	-	>250	>250	62.5–125	>125	31.2–62.5	125	31.2	125	31.2	125
A	3,5-OMe, 4-OH	>250	>250	250	>250	125–250	>250	125–250	250	125–250	>250
B	3-OMe, 4-OH	>250	>250	>250	>250	>250	>250	>250	>250	>250	>250
C	3-OH, 4-OMe	>250	>250	>250	>250	250	250	125	125	250	>250
D	2-OH	7.8–15.6	15.6	125	>250	31.2	62.5	15.6–31.2	31.2–62.5	31.2	125
E	3-OH	31.2–62.5	62.5–125	250–500	>250	250–500	>250	250	>250	125	250
F	4-OH	>250	125	>250	>250	>250	>250	250	>250	250	>250
G	2,5-OH	>250	>250	>250	>250	250	>250	250	250	250	>250

MIC = the lowest concentration of the substance that inhibited visible yeast growth.
MFC = the lowest concentration of the substances at which 99.9% of the yeasts were killed.

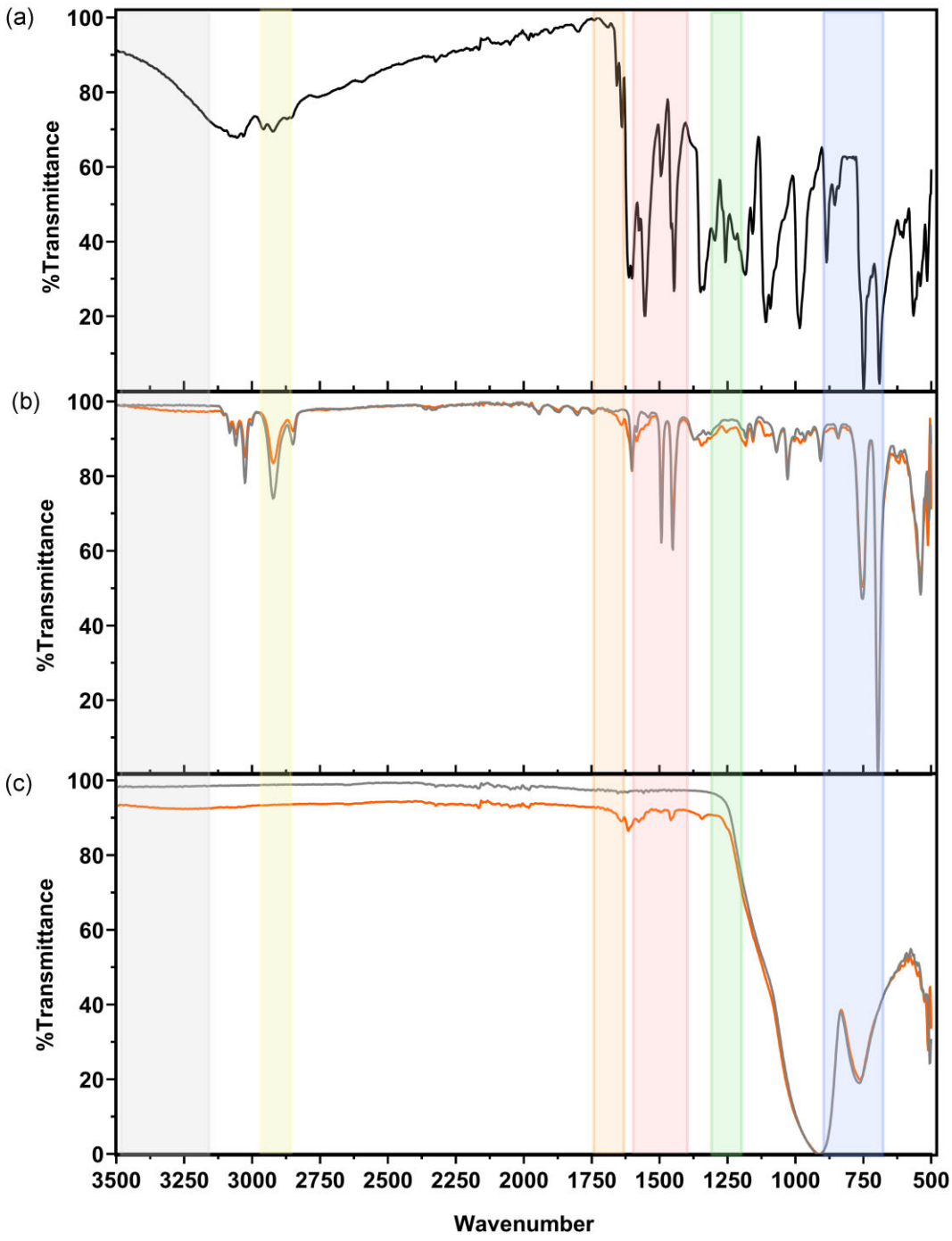

Figure 1. The FTIR spectra of curcuminoid **D** powder and coatings on polystyrene and glass. (a) powder mixed in a KBr tablet, (b) uncoated and coated polystyrene, and (c) uncoated and coated glass. The spectrum corresponding to the uncoated surfaces appears lighter (grey), while the spectrum for the curcuminoid-coated surfaces appears darker (orange). These lines may partially overlap. The coloured regions correspond to special bands in curcuminoid **D**. .

strain at concentrations below 250 μg ml^{-1}. Curcuminoid **D** had the lowest MIC and MFC values from all curcuminoid derivatives investigated. Based on these results, curcuminoid **D** was selected for further experiments.

Characterization of the curcuminoids coated surfaces

The chemical structure of curcuminoid **D** coated on polystyrene and glass surfaces was determined using FT-IR spectroscopy (Fig. 1).

The FTIR spectrum of curcuminoid **D** (Fig. 1a) showed a broad band between 3500 and 3200 cm^{-1} indicative of the O-H stretching (grey band) in the phenol group; the region between 3100 and 3000 cm^{-1} was attributed to C-H stretching (yellow band) in the aromatic ring; the region between 1750 and 1650 cm^{-1} for the conjugated C = O stretching (orange band); between 1600 and 1400 cm^{-1} the C = C stretching (red band) of the aromatic ring; between 1300 and 1200 cm^{-1} the C-O stretching (green band); and between 900 and 675 cm^{-1} the C-H bending (blue band) in the aromatic ring. This FTIR spectrum confirmed the chemical structure of curcuminoid **D**.

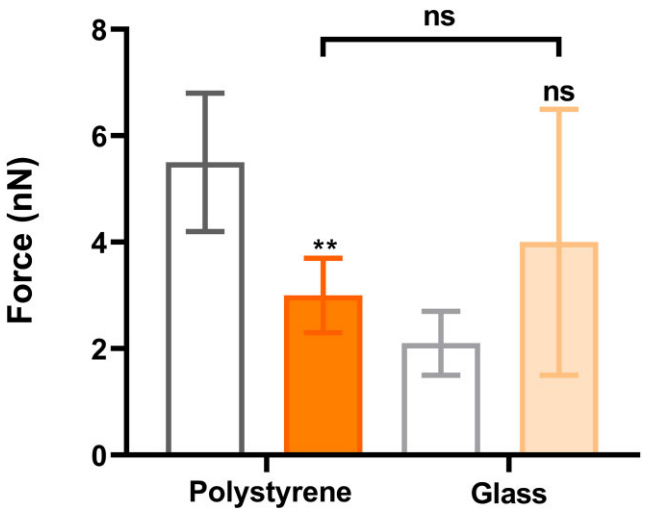

Figure 2. The effect of curcuminoid D coating on *C. albicans* ATCC 10231 adhesion strength on uncoated and curcuminoid-coated polystyrene and glass after 2 s contact. The unfilled bars are the uncoated surfaces, and the filled bars curcuminoid-coated surfaces. Data represents means ± SD of three independent experiments. Statistical analysis was performed by one-way ANOVA, and statistical significance differences between yeast adhesion strength on curcuminoid-coated and uncoated surfaces are indicated with asterisks, $**P \leq .01$.

The FTIR spectrum of coated and uncoated polystyrene (Fig. 1b) demonstrated several prominent peaks characteristic of the polymer structure, including sharp peaks corresponding to the aromatic C-H stretching vibrations (3080–3020 cm^{-1}), the aliphatic C-H stretching region (2920–2850 cm^{-1}), peaks associated with the aromatic ring C = C bonds (1600 and 1493 cm^{-1}), aromatic C-H bonds (1452 cm^{-1}), bending vibrations of the aliphatic C-H bonds from the ethyl groups (1375 cm^{-1}), and sharp peaks in the region of aromatic C-H out-of-plane bending (760–690 cm^{-1}). The spectrum of coated and uncoated glass exhibited two broad bands (Fig. 1c), the Si-O-Si stretching region (1100–1000 cm^{-1}) and around 800 cm^{-1} the Si-O stretching, which are the characteristic features of silica-based glass. Additionally, small peaks present in the coated samples at 1750–1650 cm^{-1} (orange band), at 1600–1400 cm^{-1} (red band), and 1300–1200 cm^{-1} (green band) indicate the presence of the curcuminoid **D** coating on both polystyrene and glass samples.

The wettability of the coated surfaces was determined by measuring the water contact angles. After 24 h of coating with curcuminoid **D**, the hydrophilic glass became more hydrophobic (from 0 to 51 ± 11 degrees), while the hydrophobic polystyrene did not change (from 90 ± 1 to 87 ± 3 degrees).

Adhesion strength of yeasts on curcuminoid-coated surfaces

The adhesion strength of *C. albicans* on curcuminoid-coated and uncoated polystyrene and glass surfaces was determined using AFM. The AFM data (Fig. 2) indicated that the curcuminoid **D** coating on polystyrene caused a significant 2-fold decrease in the adhesion force of *C. albicans* after 2 s in contact with the surface compared with uncoated polystyrene. The adhesion force on polystyrene was 3-fold higher than on glass, but for the curcuminoid **D** coated polystyrene and glass, the adhesion forces became very similar.

Candida albicans adhesion on the curcuminoid-coated glass in a parallel plate flow chamber

The adhesion of *C. albicans* on curcuminoid **D** coated and uncoated glass slides was evaluated in a parallel plate flow chamber. The cell adhesion on the curcuminoid-coated glass was reduced by 66% before an air-liquid interface and by 86% after an air-liquid interface when compared to the control (uncoated glass) (Fig. 3).

Effect of the curcuminoid **D** coating on *C. albicans* hyphal development

Curcuminoid **D** coating on polystyrene and glass slides inhibited the hyphal development of *C. albicans*, reducing hyphal length by 65% and 86%, respectively (Fig. 4). Longer hyphae were observed on polystyrene surfaces than on glass. On polystyrene, the average hyphal length was 75 μm, compared to 27 μm on the curcuminoid coated polystyrene, and on glass, the average hyphal length was 50 μm and 7 μm on coated glass.

Evaluation of curcuminoid coating on *C. albicans* biofilm formation

CLSM images and CFU counting (Fig. 5) indicated that curcuminoid **D** coating on polystyrene significantly inhibited the 48 h biofilm formation of *C. albicans*; however, it did not affect the biofilm formation on glass.

The curcuminoid **D** coating inhibited the formation of the cell membrane and the cell wall showing a decrease in green fluorescence by 38% and blue fluorescence by 40% when compared to the uncoated polystyrene. 3% NaOCl was used as positive control, and the treatment reduced the metabolic activity and the cell membrane by 100%, and the cell wall by 45% when compared to biofilm on uncoated polystyrene (positive control) (Fig. 5b). Furthermore, the curcuminoid **D** coating on polystyrene resulted in a 3-fold decrease in CFUs of the 48-h biofilm compared to uncoated polystyrene (Fig. 5c), while there was no effect on glass. The CFUs on coated polystyrene and glass became similar.

The metabolic activity of a 48-h-old biofilm of *C. albicans* ATCC 10231 on polystyrene was exposed to 0, 31.2, 62.5, 156, and 312 μg ml^{-1} curcuminoid **D** in growth medium for 24 h (Fig. 6). The viability of the 48 h biofilm was reduced as the concentration increased at 312 μg ml^{-1} (20 × MIC), the viability decreased 63%.

Total RNA isolation and real-time PCR

The results obtained from real-time PCR (Fig. 7) suggested that the curcuminoid **D** coating on polystyrene downregulated genes associated with biofilm formation of *C. albicans*. In the analysis of gene expression under hyphal development conditions, the gene *HWP1* (hyphal wall protein 1) was significantly downregulated on coated surfaces, with a 15-fold reduction compared to uncoated surfaces. During the initial 2 h biofilm formation on curcuminoid-coated surfaces, genes from the ALS family, responsible for the adhesins, as *ALS3* (agglutinin-like sequence 3), *ALS5* (agglutinin-like sequence 5), and *HWP1* were significantly downregulated by 20-fold, 3-fold, and 13-fold, respectively, when compared with uncoated surfaces. Notably, at the 48 h biofilm, *ALS1* expression was significantly upregulated on coated surfaces, showing a 5-fold

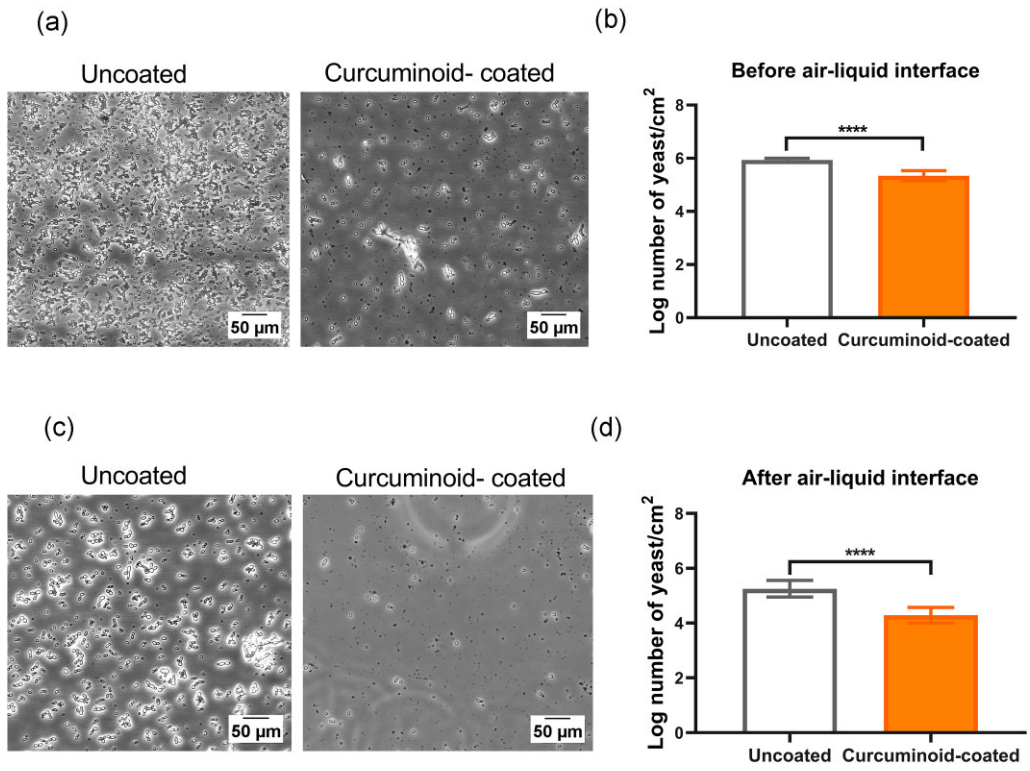

Figure 3. The effect of curcuminoid **D** coating on glass on the adhesion of *C. albicans* ATCC 10231 in a parallel plate flow chamber before (a, b) and after an air-liquid interface (c, d). Data represent means ± SD of three independent experiments. Statistical analysis was performed by Student's *t*-test, and statistical significance between yeast density on curcuminoid-coated and uncoated surfaces is indicated with asterisks, ****$P \leq .0001$.

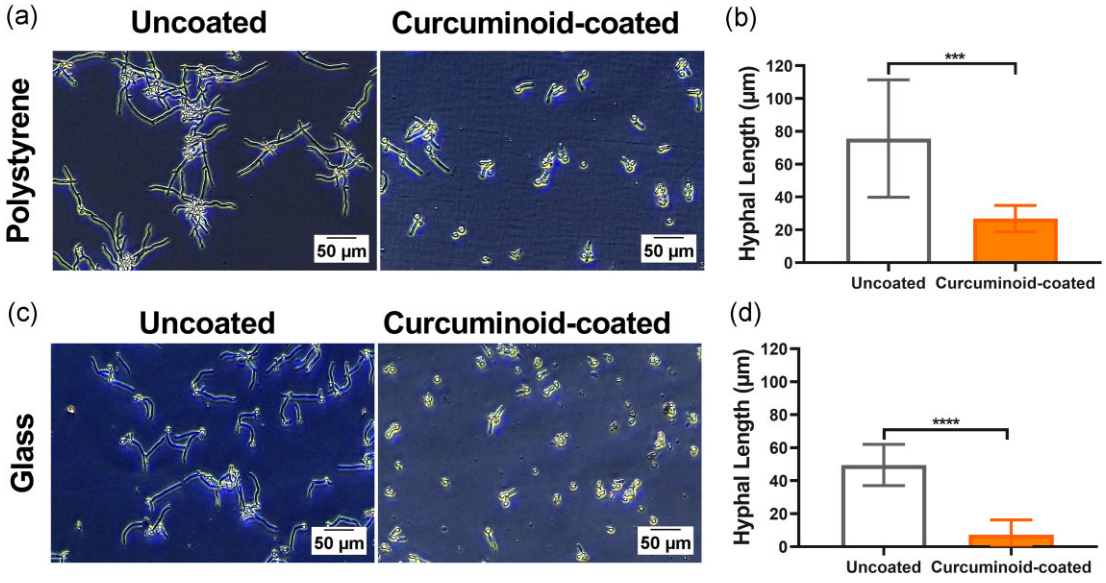

Figure 4. Effect of curcuminoid D coating on polystyrene (a, b) and glass (c, d) on the development of the hyphal length of *C. albicans* ATCC 10231. Data represent means ± SD of three independent experiments. Statistical analysis was performed by Student's *t*-test, and statistical significance between hyphal development length on curcuminoid-coated and uncoated surfaces is indicated with asterisks, ***$P \leq .001$ and **** $P \leq .0001$.

increase compared to uncoated surfaces. These findings indicate that the coating significantly inhibits gene expression essential for initial fungal biofilm development and adhesion while potentially enhancing genes involved in later stages of biofilm maturation.

Cytotoxicity of curcuminoid-coated surfaces

The viability of HGF-1 and HOK cells was not significantly affected by exposure to curcuminoid-coated surfaces compared to uncoated controls. The curcuminoid was slightly toxic to the more sensitive primary HOK cells but still above the 70%

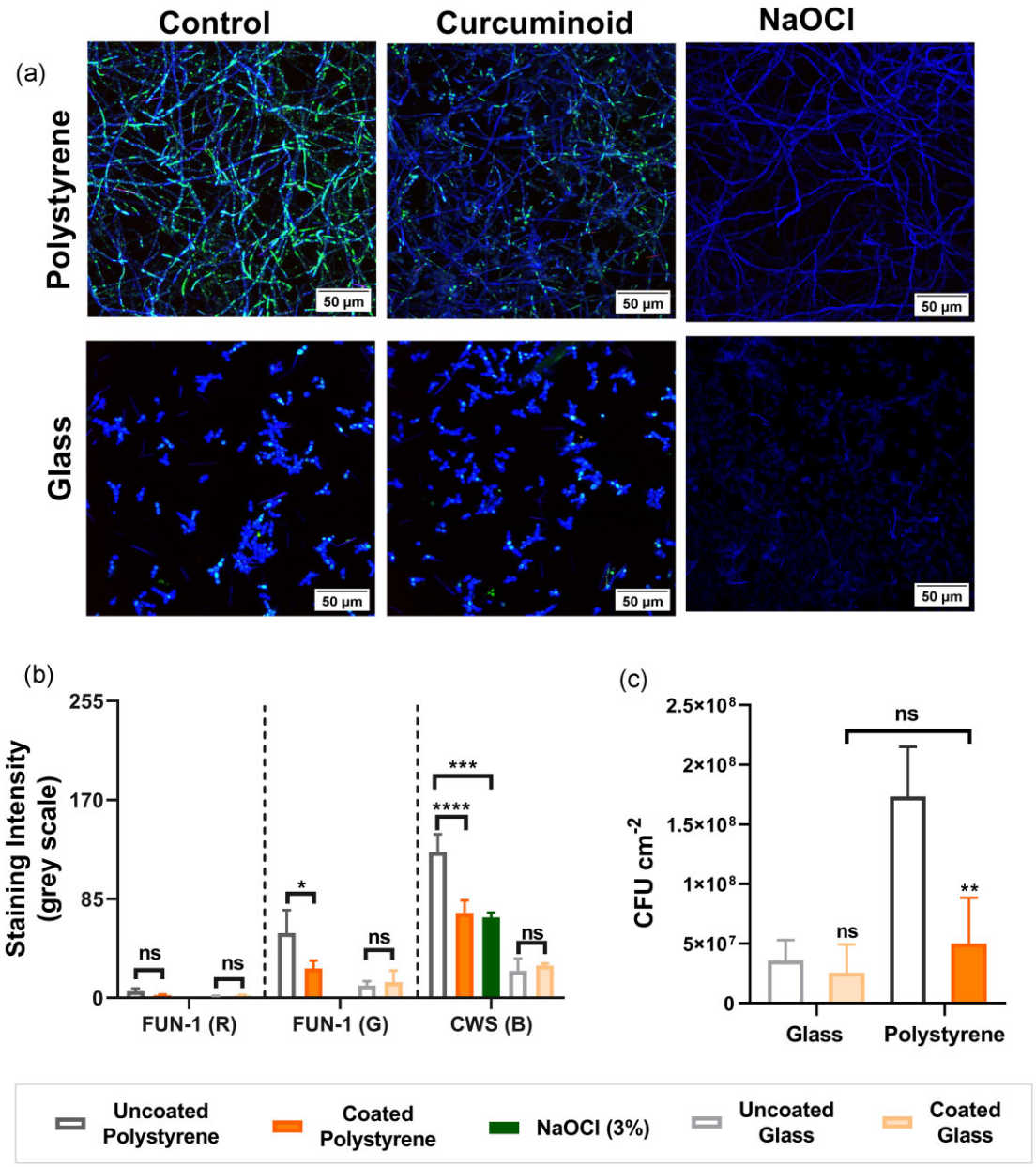

Figure 5. (a) Representative CLSM images of 48 h biofilms of *C. albicans* ATCC 10231 grown on uncoated and curcuminoid-coated polystyrene and glass. The effect of the curcuminoid coating on metabolically active intravacuolar structures [red-fluorescent, FUN-1 (R)], cell membrane [green-fluorescent, FUN-1 (G)], and cell wall [blue-fluorescent, CWS (B)]. NaOCl (3%) exposure for 30 s was used as a positive control. (b) Quantitative fluorescence intensity of the CLSM images in panel a. (c) Effect of curcuminoid **D** coating on 48 h biofilm formation of *C. albicans* ATCC 10231 expressed by CFU per cm^2. Data represents means ± SD of three independent experiments.

viability, which is in accordance with ISO 10993-5 standards (Fig. 8).

Discussion

In this study, we developed and evaluated the use of a monocarbonyl curcuminoid as a coating to inhibit biofilm formation of *C. albicans*. Seven monocarbonyl curcuminoids were evaluated for their anti-*Candida* activity (see Table 1). Among these compounds, curcuminoid **D** showed the most potent anti-*Candida* activity, exhibiting fungicidal effects against all tested *Candida* species, with MFC values ranging from 15.6 to 125 µg ml^{-1}. The observed differences in MIC and MFC values among *C. albicans* strains likely stem from inherent, strain-specific characteristics. Differences in genetic background can influence gene expression and regulatory mechanisms, resulting in variable antifungal susceptibility and resistance. A study showed that genetically distinct *C. albicans* strains exposed to fluconazole developed diverse adaptive responses, including variations in drug tolerance and genome size, underscoring the critical role of genetic background in shaping resistance profiles (McTaggart et al. 2020).

The presence of a hydroxyl group at the 2′ position in curcuminoid **D** significantly enhanced its anti-*Candida* activity, exceeding other structural modifications and curcumin (Table 2). Previous studies reported MIC values for curcumin

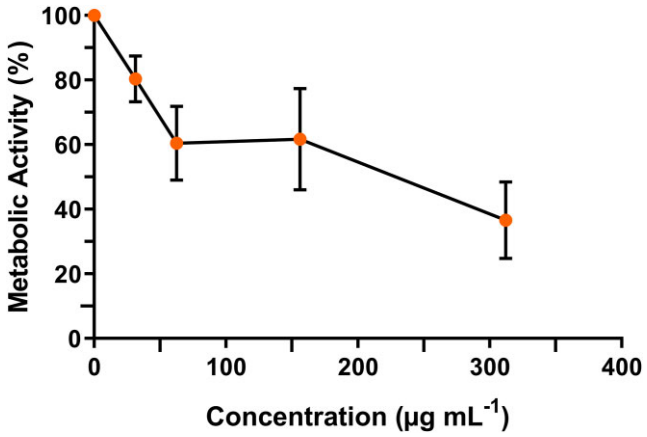

Figure 6. A 48 h biofilm of *C. albicans* ATCC 10231 exposed to different concentrations curcuminoid **D** evaluated by the metabolic activity using MTT reduction assay.

ranging from 100 to 2000 μg ml^{-1} against planktonic *C. albicans* (Alalwan et al. 2017, Shahzad et al. 2014), which is similar as our results (Table 2), except for curcuminoid **D**, which had a lower MIC.

Adhesion force measurements demonstrated that curcuminoid D coatings on polystyrene surfaces significantly reduced *C. albicans* adhesion force compared to uncoated surfaces and became similar as the adhesion force on coated glass (Fig. 2). While water contact angle measurements showed that curcuminoid D increased the hydrophobicity of glass but had no effect on polystyrene, the significant difference in wettability between the two coated surfaces suggests that the reduction in adhesion force is due to direct interaction of the coating with *C. albicans*, rather than being influenced by the wettability of the surfaces.

Curcuminoid **D** disrupts *C. albicans* cell membrane and cell wall, weakening the structural components essential for adhesion, as evidenced by a decreased adhesion force and reduced adhesion under flow conditions (Fig. 3). This disruption also impairs biofilm formation, as indicated by the significant reduction in CFUs of the 48-h biofilm. CLSM results further support this, showing that curcuminoid **D** coating significantly inhibited the formation of the cell membrane and cell wall (Fig. 5). Despite structural differences between curcuminoid **D** and curcumin (Lee and Lee 2014), we can draw comparisons with curcumin and other curcuminoids that target similar pathways. Curcumin and monocarbonyl curcuminoid have been shown to disrupt fungal cell membranes by interfering with ergosterol (Lee and Lee 2014, Polaquini et al. 2024). Molecular docking studies on quinoline-based monocarbonyl curcumin analogues further support this mechanism, demonstrating that these molecules bind within the active site of 14α-demethylase (Nagargoje et al. 2020a). Specifically, hydrogen bonding between the carbonyl group of the curcuminoid and the tyrosine of the enzyme, along with π–π stacking interactions between the benzene rings of the curcuminoid and histidine residues. This interaction inhibits 14α-demethylase from converting lanosterol into ergosterol, thereby impairing ergosterol synthesis and destabilizing the fungal membrane (Nagargoje et al. 2020a). Regarding the cell wall, curcumin's disruptive activity in *C. albicans* has been linked to its interference with the calcineurin signalling pathway (Kumar et al. 2014).

Another investigated mechanism was the ability of curcuminoid **D** to inhibit the transition from yeast-form to hyphal-

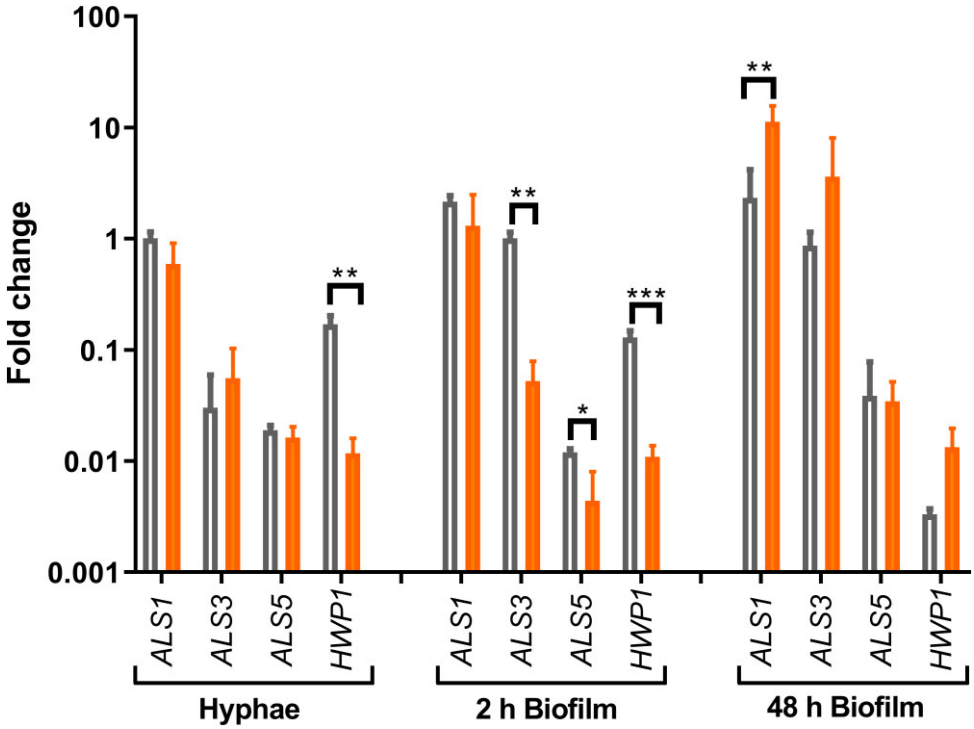

Figure 7. Gene expression of *C. albicans* ATCC 10231 biofilm during different stages of biofilm formation of *C. albicans* hyphal development, 2 and 48 h biofilm on uncoated and curcuminoid-coated polystyrene. *ALS1*, *ALS3*, and *ALS5* genes: agglutinin-like sequence; *HWP1* gene: hyphae cell wall protein. All data are represented relative to fold changes compared to *ACT1* housekeeping gene. The unfilled bar corresponds to the uncoated surfaces and the filled bar to the curcuminoid-coated surfaces. The standard bar error represents the mean of three replicates.

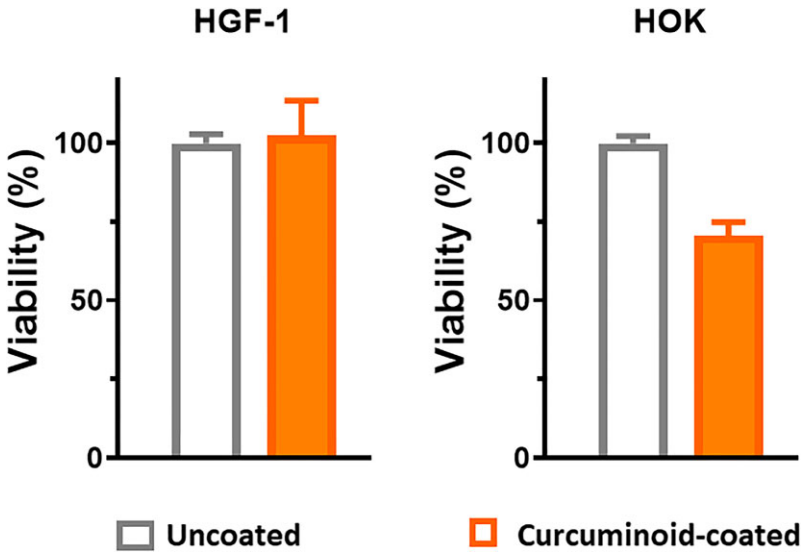

Figure 8. Viability of human gingival fibroblast (HGF-1) and human oral keratinocytes (HOK) on curcuminoid-coated polystyrene surfaces. The standard bar error represents the mean of three replicates.

form, an important virulence factor and essential for adhesion and a critical step in biofilm formation. Curcuminoid **D** effectively inhibited this morphological transition on both glass and polystyrene surfaces (Fig. 4). Notably, a variability in hyphal length was observed on the uncoated polystyrene surface, which may be attributed to a different growth phase of the hyphae (Berman 2006) or the microscale heterogeneity inherent to polystyrene substrates (Rosado-Galindo and Domenech 2020). Microscale variations in topography can influence local adhesion, nutrient availability, and microenvironmental conditions, ultimately affecting cell differentiation and elongation (Rosado-Galindo and Domenech 2020). Furthermore, without a coating to modulate surface properties, cells may interact with the substrate in a less uniform manner.

The interference of curcuminoid **D** in the morphological differentiation of *C. albicans* was confirmed by the downregulation of the *HWP1* gene on coated surfaces (Fig. 7). *HWP1* gene encodes a hypha-specific cell wall protein that plays a crucial role in adhesion during filamentation and is essential for biofilm maturation (Nobile et al. 2006). Additionally, the coating suppressed the expression of *ALS3* and *ALS5*, two members of the agglutinin-like sequence (ALS) gene family. *ALS3* is involved in strong adhesion to epithelial cells and abiotic surfaces and facilitates host cell invasion (Liu and Filler 2011), whereas *ALS5* is associated with initial attachment and maintaining biofilm integrity (Atriwal et al. 2021). These gene expression changes are consistent with previous reports indicating that inhibition or deletion of these genes results in diminished biofilm formation (Atriwal et al. 2021, Garcia et al. 2011, Liu and Filler 2011). The combined results demonstrated that the coating effectively impeded hyphal development, adhesion and reduced biofilm formation.

Here, we demonstrated that curcuminoid D effectively impeded fungal adhesion, hyphal development, biofilm formation, reduced the metabolic activity of mature biofilms (Fig. 6) and is not cytotoxic, making it a promising candidate for surface modification.

Compared to other antifungal surface coatings, curcuminoid D offers several advantages. Silver-based coatings, while effective against yeasts, pose risks of cytotoxicity and resistance due to silver ion release (Duval et al. 2019, Thapliyal et al. 2025). Chitosan coatings, which are biocompatible and biodegradable, often exhibit limited mechanical stability, and the antifungal efficacy largely depends on pH, solubility, and environmental degradation (Kumari et al. 2021). Additionally, natural curcumin-based coatings rely on sustained release formulations, which can cause fluctuating antifungal activity and reduced long-term effectiveness (Sohn et al. 2021).

Other studies have shown that curcumin can degrade in <24 h under various conditions as e.g. degradation of 60% was reached in 1 h and over 90% in 4 h when exposed to light in phosphate buffer (pH = 7.2) (Appendino et al. 2022). Incubating curcumin with proteins, such as in the presence of serum or cultured cells, increased the half-life time of curcumin, although this increase was limited to 1–2 h (Schneider et al. 2015). In contrast, our curcuminoid D coating demonstrated sustained antifungal activity for at least 48 h and did not show cytotoxic effects on human cells. Its multifaceted mechanism of action targets key fungal components, including membrane disruption, inhibition of adhesion-related gene expression, and interference with cell wall integrity, making it a promising alternative for coating applications, offering enhanced stability and efficacy. While the sustained activity is encouraging, it is important to note that no quantitative assessment of coating leaching or long-term stability was performed in this study. Future studies should focus on assays to evaluate coating integrity under physiological conditions to better understand its durability and efficacy over time.

This study underscores the potential of monocarbonyl curcuminoids as an antimicrobial coating to prevent biofilm formation, offering a promising strategy for biofilm control in clinical applications, such as voice prostheses. Patients with silicone rubber voice prostheses often develop thick, mixed-species biofilms of yeast and bacteria, which penetrate into the silicone rubber and lead to speech difficulties and leakage (Neu et al. 1993). *C. albicans* hyphal formation plays a crucial role in this deterioration (Oosterhof et al. 2006, Van Weissenbruch et al. 1997), making it a key target for interven-

tion. Inhibiting hyphal growth could significantly extend the lifetime of voice prostheses and improve patient outcomes.

A limitation of this study is the predominant use of *C. albicans* ATCC 10231 as the model strain. While this well-characterized reference strain allows for reproducibility, it may not fully reflect the variability observed among clinical isolates. Such strains can differ in adhesion properties, resistance profiles, and pathogenicity depending on the infection site and patient background. Future work will need to incorporate a broader panel of clinical and drug-resistant isolates to enhance the translational clinical relevance of the findings.

Conclusion

This study highlighted the potential of monocarbonyl curcuminoids as an antimicrobial coating. Curcuminoid **D** (2-hydroxy-dibenzylideneacetone) demonstrated potent anti-*Candida* activity, effectively inhibiting fungal adhesion, hyphal development, biofilm formation and no cytotoxicity on polystyrene surfaces. Gene expression analysis confirmed downregulation of the key adhesion and biofilm-related genes. Although its efficacy on glass was limited over 48 h, the coating still reduced adhesion and hyphal development. These findings evidenced the role of monocarbonyl curcuminoids as multifaceted coatings for controlling device-associated infections and biofilm formation in clinical settings.

Acknowledgements

The authors thank Jelly Atema-Smit and Gésinda Geertsema-Doornbusch for training and technical help on the flow chamber, Willem Woudstra for the training and technical help on confocal and FT-IR analysis, Joop de Vries for technical support related to AFM, Willy de Haan-Visser, Emma Dijkstra, and Paulien Schaafsma for training and technical help on RT-PCR, Lu Yuan for cytotoxicity measurements.

The authors gratefully acknowledge financial support from the Department of Biomaterials & Biomedical Technology, University Medical Center Groningen.

Author contributions

Veridianna C. Pattini (Conceptualization, Data curation, Formal Analysis, Investigation, Methodology, Validation, Writing – original draft, Writing – review & editing), Leticia R. de Assis (Data curation, Investigation, Writing – review & editing), Margarete T. G. de Almeida (Conceptualization, Formal Analysis, Supervision, Writing – review & editing), Luis O. Regasini (Conceptualization, Formal Analysis, Funding acquisition, Project administration, Supervision, Validation, Writing – review & editing), and Henny C. van der Mei (Conceptualization, Formal Analysis, Funding acquisition, Project administration, Resources, Supervision, Validation, Writing – original draft, Writing – review & editing).

Supplementary data

Supplementary data is available at *JAMBIO Journal* online.

Conflict of interest: None declared.

Funding

This study was financed in part by the Coordination for the Improvement of Higher Education Personnel - Brazil (CAPES) - Finance Code 001 and the Abel Tasman Talent Program - University of Groningen.

Data availability

Data will be shared on request.

References

Abreu AC, Tavares RR, Borges A *et al*. Current and emergent strategies for disinfection of hospital environments. *J Antimicrob Chemother* 2013;**68**:2718–32. https://doi.org/10.1093/jac/dkt281

Afewerki S, Bassous N, Harb S *et al*. Advances in antimicrobial and osteoinductive biomaterials. In: Li B, Moriarty T, Webster T, Xing M (eds.), *Racing for the Surface*. Cham: Springer International Publishing, 2020, 3–34. https://doi.org/10.1007/978-3-030-34471-9

Alalwan H, Rajendran R, Lappin DF *et al*. The anti-adhesive effect of curcumin on *Candida albicans* biofilms on denture materials. *Front Microbiol* 2017;**8**:669. https://doi.org/10.3389/fmicb.2017.00659

Alves D, Vaz AT, Grainha T *et al*. Design of an antifungal surface embedding liposomal amphotericin B through a mussel adhesive-inspired coating strategy. *Front Chem* 2019;**7**:431. https://doi.org/10.3389/fchem.2019.00431

Appendino G, Allegrini P, de Combarieu E *et al*. Shedding light on curcumin stability. *Fitoterapia* 2022;**156**:105084. https://doi.org/10.1016/j.fitote.2021.105084

Atriwal T, Azeem K, Husain FM *et al*. Mechanistic understanding of *Candida albicans* biofilm formation and approaches for its inhibition. *Front Microbiol* 2021;**12**:638609. https://doi.org/10.3389/fmicb.2021.638609

Berman J. Morphogenesis and cell cycle progression in *Candida albicans*. *Curr Opin Microbiol* 2006;**9**:595–601. https://doi.org/10.1016/j.mib.2006.10.007

Busscher HJ, Van Der Mei HC. Microbial adhesion in flow displacement systems. *Clin Microbiol Rev* 2006;**19**:127–41. https://doi.org/10.1128/CMR.19.1.127-141.2006

Campoccia D, Montanaro L, Arciola CR. A review of the biomaterials technologies for infection-resistant surfaces. *Biomaterials* 2013;**34**:8533–54. https://doi.org/10.1016/j.biomaterials.2013.07.089

Carniello V, Peterson BW, Van der Mei H *et al*. Role of adhesion forces in mechanosensitive channel gating in *Staphylococcus aureus* adhering to surfaces *npj Biofilms Microbiomes* 2020;**6**:31. https://doi.org/10.1038/s41522-020-00141-z

CLSI. Reference method for broth dilution antifungal susceptibility testing of yeasts; approved standard—Third Edition. *CLSI Document M27-A3*, 2008.

Dai F, Liu GY, Li Y *et al*. Insights into the importance for designing curcumin-inspired anticancer agents by a prooxidant strategy: the case of diarylpentanoids. *Free Radical Biol Med* 2015;**85**:127–37. https://doi.org/10.1016/j.freeradbiomed.2015.04.017

Duval RE, Gouyau J, Lamouroux E. Limitations of recent studies dealing with the antibacterial properties of silver nanoparticles: fact and opinion. *Nanomaterials* 2019;**9**:1775. https://doi.org/10.3390/nano9121775

Garcia MC, Lee JT, Ramsook CB *et al*. A role for amyloid in cell aggregation and biofilm formation. *PLoS One* 2011;**6**:e17632. https://doi.org/10.1371/journal.pone.0017632

Gaydhane MK, Kanuganti JS, Sharma CS. Honey and curcumin loaded multilayered polyvinylalcohol/cellulose acetate electrospun nanofibrous mat for wound healing. *J Mater Res* 2020;**35**:600–9. https://doi.org/10.1557/jmr.2020.52

Kumar A, Dhamgaye S, Maurya IK *et al*. Curcumin targets cell wall integrity via calcineurin-mediated signaling in *Candida albicans*. *An-*

timicrob Agents Chemother 2014;**58**:167–75. https://doi.org/10.1128/AAC.01385-13
Kumari S, Tiyyagura HR, Pottathara YB *et al*. Surface functionalization of chitosan as a coating material for orthopaedic applications: a comprehensive review. *Carbohydr Polym* 2021;**255**:117487. https://doi.org/10.1016/j.carbpol.2020.117487
Lamont-Friedrich SJ, Kidd SE, Giles C *et al*. *Candida auris* susceptibility on surfaces coated with the antifungal drug caspofungin. *Med Mycol* 2021;**60**:myab075. https://doi.org/10.1093/mmy/myab075
Lee W, Lee DG. An antifungal mechanism of curcumin lies in membrane-targeted action within *Candida albicans*. *IUBMB Life* 2014;**66**:780–5. https://doi.org/10.1002/iub.1326
Liu Y, Filler SG. *Candida albicans* Als3, a multifunctional adhesin and invasin. *Euk Cell* 2011;**10**:168–73. https://doi.org/10.1128/EC.00279-10
Magill SS, Edwards JR, Bamberg W *et al*. Multistate point-prevalence survey of health care–associated infections. *N Engl J Med* 2014;**370**:1198–208. https://doi.org/10.1056/NEJMoa1306801
Manohar CM, Prabhawathi V, Sivakumar PM *et al*. Design of a papain immobilized antimicrobial food package with curcumin as a crosslinker. *PLoS One* 2015;**10**:1–17. https://doi.org/10.1371/journal.pone.0121665
McTaggart LR, Cabrera A, Cronin K *et al*. Antifungal susceptibility of clinical yeast isolates from a large Canadian reference laboratory and application of whole-genome sequence analysis to elucidate mechanisms of acquired resistance. *Antimicrob Agents Chemother* 2020;**64**:e00402–20. https://doi.org/10.1128/AAC.00402-20
Modak SM, Ghosh AK, De Silva CC *et al*. Coatings and methods for infection-resistant medical devices. U.S. Patent Application US20190133126A1. 2019, 1–26.
Naderi J, Giles C, Saboohi S *et al*. Combatting fungal biofilm formation by diffusive release of fluconazole from heptylamine plasma polymer coating. *Biointerphases* 2020;**15**:061012. https://doi.org/10.1116/6.0000511
Nagargoje AA, Akolkar SV, Siddiqui MM *et al*. Quinoline based monocarbonyl curcumin analogs as potential antifungal and antioxidant agents: synthesis, bioevaluation and molecular docking study. *Chem Biodivr* 2020a;**17**:e1900624. https://doi.org/10.1002/cbdv.201900624
Nagargoje AA, Akolkar SV, Subhedar DD *et al*. Propargylated monocarbonyl curcumin analogues: synthesis, bioevaluation and molecular docking study. *Med Chem Res* 2020b;**29**:1902–13. https://doi.org/10.1007/s00044-020-02611-7
Nelson KM, Dahlin JL, Bisson J *et al*. The essential medicinal chemistry of curcumin. *J Med Chem* 2017;**60**:1620–37. https://doi.org/10.1021/acs.jmedchem.6b00975
Neu TR, Van der Mei HC, Busscher HJ *et al*. Biodeterioration of medical-grade silicone rubber used for voice prostheses: a SEM study. *Biomaterials* 1993;**14**:459–64. https://doi.org/10.1016/0142-9612(93)90149-V
Nobile CJ, Nett JE, Andes DR *et al*. Function of *Candida albicans* adhesin HWP1 in biofilm formation. *Euk Cell* 2006;**5**:1604–10. https://doi.org/10.1128/EC.00194-06
Oosterhof JJH, Buijssen KJDA, Busscher HJ *et al*. Effects of quaternary ammonium silane coatings on mixed fungal and bacterial biofilms on tracheoesophageal shunt prostheses. *Appl Environ Microb* 2006;**72**:3673–7. 3677https://doi.org/.2006
Pfaller MA, Diekema DJ. Epidemiology of invasive candidiasis: a persistent public health problem. *Clin Microbiol Rev* 2007;**20**:133–63. https://doi.org/10.1128/CMR.00029-06
Polaquini C, Sardi J, Pattini V *et al*. Design, synthesis and anti-*Candida* activity of diarylideneacetones inspired by curcumin. *SSRN* 2024. Available at: http://dx.doi.org/10.2139/ssrn.4785660 *(3 June 2025, date last accessed)*.
Polaquini CR, Marques BC, Ayusso GM *et al*. Antibacterial activity of a new monocarbonyl analog of curcumin MAC 4 is associated with divisome disruption. *Bioorg Chem* 2021;**109**:104668. https://doi.org/10.1016/j.bioorg.2021.104668
Rosado-Galindo H, Domenech M. Polystyrene topography sticker array for cell-based assays. *Rpm* 2020;**2**:1–18. https://doi.org/10.21926/rpm.2002013
Schneider C, Gordon ON, Edwards RL *et al*. Degradation of curcumin: from mechanism to biological implications. *J Agric Food Chem* 2015;**63**:7606–14. https://doi.org/10.1021/acs.jafc.5b00244
Shahzad M, Sherry L, Rajendran R *et al*. Utilising polyphenols for the clinical management of *Candida albicans* biofilms. *Int J Antimicrob Agents* 2014;**44**:269–73. https://doi.org/10.1016/j.ijantimicag.2014.05.017
Shen T, Jiang T, Long M *et al*. A curcumin derivative that inhibits vinyl carbamate-induced lung carcinogenesis via activation of the Nrf2 protective response. *Antioxid Redox Signaling* 2015;**23**:651–64. https://doi.org/10.1089/ars.2014.6074
Shetty D, Kim Y, Shim H *et al*. Eliminating the heart from the curcumin molecule: monocarbonyl curcumin mimics (MACs). *Molecules* 2014;**20**:249–92. https://doi.org/10.3390/molecules20010249
Singh AK, Gaur V, Maurya AK. The role of biofilm in originating, mediating, and proliferating infectious diseases. In: Kumar S, Chandra N, Singh L *et al*. (eds.), *Biofilms in Human Diseases: Treatment and Control*. Cham: Springer; 2019, 43–57. https://doi.org/10.1007/978-3-030-30757-8
Sohn S-I, Priya A, Balasubramaniam B *et al*. Biomedical applications and bioavailability of curcumin—an updated overview. *Pharmaceutics* 2021;**13**:2102. https://doi.org/10.3390/pharmaceutics13122102
Srivastava A, Chandra N, Kumar S. The role of biofilms in medical devices and implants. In: Kumar S, Chandra N, Singh L *et al*. (eds.), *Biofilms in Human Diseases: Treatment and Contro*. Cham: Springer; 2019, 151–65. https://doi.org/10.1007/978-3-030-30757-8
Sunitha S, Adinarayana K, Pankaj T *et al*. Fabrication of surgical sutures coated with curcumin loaded gold nanoparticles. *Pharm Anal Acta* 2017;**08**:529. https://doi.org/10.4172/2153-2435.1000529
Thapliyal D, Verros GD, Arya RK. Nanoparticle-doped antibacterial and antifungal coatings. *Polymers* 2025;**17**:247. https://doi.org/10.3390/polym17020247
Van Weissenbruch R, Albers FWJ, Bouckaert S *et al*. Deterioration of the provox TM silicone tracheoesophageal voice prosthesis: microbial aspects and structural changes. *Acta Otolaryngol* 1997;**117**:452–8. https://doi.org/10.3109/00016489709113420
Virk RS, Rehman MAU, Munawar MA *et al*. Curcumin-containing orthopedic implant coatings deposited on polyether-ether-ketone/bioactive glass/hexagonal boron nitride layers by electrophoretic deposition. *Coatings* 2019;**9**:572. https://doi.org/10.3390/coatings9090572
Weber WM, Hunsaker LA, Abcouwer SF *et al*. Anti-oxidant activities of curcumin and related enones. *Bioorg Med Chem* 2005;**13**:3811–20. https://doi.org/10.1016/j.bmc.2005.03.035
Zhou J, Tao Q-Q, Wang P-Y *et al*. Antimicrobial evaluation and action mechanism of pyridinium-decorated 1,4-pentadien-3-one derivatives. *Bioorg Med Chem Lett* 2018;**28**:1742–6. https://doi.org/10.1016/j.bmcl.2018.04.034

Received 3 April 2025; **revised** 4 June 2025; **accepted** 22 June 2025